Casimir effects for a flat plasma sheet: II. Fields and stresses

2005 J. Phys. A: Math. Gen. 38 3021

(http://iopscience.iop.org/0305-4470/38/13/014)

INSTITUTE OF PHYSICS PUBLISHING JOURNAL OF PHYSICS A: MATHEMATICAL AND GENERAL

J. Phys. A: Math. Gen. **38** (2005) 3021–3044 doi:10.1088/0305-4470/38/13/014

Casimir effects for a flat plasma sheet: II. Fields and stresses

G Barton

Department of Physics and Astronomy, University of Sussex, Brighton BN1 9QH, UK

Received 20 October 2004, in final form 5 January 2005
Published 14 March 2005
Online at stacks.iop.org/JPhysA/38/3021

Abstract

We study the self-stresses experienced by the single plasma sheet modelled in the preceding paper, and determine the exact mean-squared Maxwell fields in vacuum around it. These are effects that probe the physics of such systems further than do the ground-state eigenvalues responsible for the cohesive energy β; in particular, unlike β they depend not only on the collective properties but also on the self-fields of the charge carriers. The classical part of the interaction between the sheet and a slowly moving charged particle follows as a byproduct. The main object is to illustrate, in simple closed or almost closed form, the consequences of imperfect (dispersive) reflectivity. The largely artificial limit of perfect reflection reduces all the results to those long familiar outside a half-space taken to reflect perfectly from the outset; but a careful examination of the approach to this limit is needed in order to resolve paradoxes associated with the surface energy, and with the mechanism which, in the limit, disjoins the two flanking half-spaces both electromagnetically and quantally.

PACS numbers: 03.65.−w, 03.70.+k, 11.10.−z, 12.20.−m, 36.40.Gk, 42.50.Pq

1. Introduction

1.1. Background and motivation

The preceding paper (Barton 2005, referred to as B.V) determined the cohesive Casimir energies β for a simple fluid model of an infinitesimally thin flat plasma sheet occupying the xy plane. Here we extend this study to some effects governed directly by the Maxwell fields, which reveal more of the physics than could be learned merely through the ground-state energy eigenvalues. The model was introduced in B.V, whose sections 1 and 2 are taken as read. We recall that the fluid has charge and mass e/a^2, m/a^2 per unit area, and define a dimensionless distance ζ in terms of the coupling-strength parameter q:

$$q \equiv 2\pi e^2/mc^2a^2 = 2\pi r_0/a^2, \qquad \zeta \equiv 2qz. \tag{1.1}$$

From the mean-squared fields (and from any energy densities or energies that may enter the discussion) we drop, as in B.V, the components that would be present even if the sheet were not. They are recognized as those surviving in the limit $z \to \infty$, i.e. as the terms independent of z. For convenience we call this step the *vacuum subtraction*. Presently we shall see that, perhaps paradoxically, it is not always equivalent to dropping terms formally of order q^0.

Switching the investigation to the fields requires three major shifts in one's point of view. They concern (i) the so-called Born subtractions which link β to the total energy (B.V, sections 3.1 and 3.3.1); (ii) the role of the odd-parity normal modes, which are affected by the sheet only through their overall phase (B.V, section 2.2), and are thereby irrelevant to β, but which remain fully effective regarding the fields; and (iii) the Debye cutoff $K \sim 1/a$ on surface-parallel wavenumbers k, essential to β, but for our present purposes demonstrably inappropriate.

(i) *The Born subtractions* remove, from the total energy of the sheet, the components of order q, identified in B.III (Barton 2004a) and again in B.V as the self-energies of the charge carriers, i.e. the self-energy of the given amount of fluid but at infinite dilution. These are manifestly irrelevant to β. But to the Maxwell fields in vacuo (nonzero z) the self-fields of the fluid contribute in full, whence Born subtractions are not required and not allowed.

(ii) *Odd- and even-parity modes must now be treated on an exactly equal footing,* in spite of the fact that the amplitudes of the odd modes do not explicitly feature the coupling strength q at all. The most forceful if not physically the most fastidious demonstration considers the perfect-reflector limit $q \to \infty$ (appendix F), where the two parities contribute equally to the mean-square fields: dropping the odd-parity modes (as if the vacuum subtraction were misinterpreted as a blanket prescription to drop terms of order q^0) one would be left with only half the archetypal expressions (F.6). Similarly absurd conclusions follow, albeit very laboriously, for finite q.

(iii) Finally, except for a few asides in the appendices, we shall *dispense with cutoffs, i.e. admit all values of k*. While a Debye cutoff is unquestionably proper to effects governed, like β, by the collective properties of the sheet, it is unwarranted for the effects we propose to study, which depend also on the self-fields. Other types of cutoff might perhaps emerge from some future adaptation of a fully relativistic theory, giving mutually consistent rules for contributions from self-fields and from collective modes (like our surface modes). But such rules would have to differ drastically from a blanket restriction $k \leqslant K \sim O(1/a)$, seeing that a harks back to the *spacing* between the charge carriers of some underlying granular material. For instance, it would plainly be absurd to impose a simple Debye-type condition on the odd-parity modes, which have no explicit dependence at all on the interaction parameter q.

Points (i) and (iii) are coupled through the fact that our model produces most answers as integrals over k. Born subtractions soften the integrands at infinity, making the end result for β less sensitive to large $k \gtrsim 1/a$, and by implication to small $z \lesssim a$, than it would have been unsubtracted. In particular this is true for the energy density u residing in the Maxwell field, i.e. off the sheet, and for its integral U:

$$u(z) \equiv \langle \mathbf{E}^2 + \mathbf{B}^2 \rangle / 8\pi, \qquad U \equiv 2 \int_0^\infty \mathrm{d}z\, u, \tag{1.2}$$

where $\langle \cdots \rangle$ denotes exact ground-state expectation values. Thus, though a cutoff is essential for convergence, β is relatively insensitive to its finer details. Conversely, *the unsubtracted expression for u is trustworthy at best for* $z \gtrsim a$. For smaller z it is quite strongly model dependent; any naive exclusion of $k > K$ would distort u ($z \lesssim a$) out of all recognition; and

rather than try to speculate blindly about more plausible cutoffs, it seems better to proceed without any at all, pending eventual improvement through more realistic models.

Accordingly, we shall simply disregard density components proportional to $\delta(z)$: they are unobservable off the sheet, and irrelevant to the in principle measurable energy β already known from B.V. By the same token we now can, and must, tolerate components diverging nonintegrably as $z \to 0$. Examples occur, respectively, in appendix F.1.1, and throughout section 3.

To illustrate the importance of clarity on such questions, we recall that in principle $\langle \mathbf{E}^2 \rangle$ say is measurable via the Casimir–Polder approximation $V_{\rm CP}$ to the potential V between the sheet and an atom at a distance z:

$$V \underset{z/\Lambda \gg 1}{\to} -\frac{1}{2}\Pi \langle \mathbf{E}^2 \rangle \underset{\zeta \gg 1}{\to} V_{\rm CP} \equiv -\frac{3\hbar c \Pi}{8\pi z^4}, \tag{1.3}$$

where Π is the electrostatic polarizability of the atom, Λ is of the order of its dominant absorption wavelengths, and where we have anticipated the results of section 3 for $\lim_{\zeta\to\infty}\langle \mathbf{E}^2 \rangle$.

In brief, the body of this paper dispenses with cutoffs altogether. But a Debye cutoff will be re-admitted temporarily in some of the appendices, in cases where there is scope for comparing the results for finite K with expressions already ensconced in the literature on other models. Such calculations will require the precise definitions of K, of the dimensionless ratio X (B.V, section 2.1) and of a second dimensionless distance Z:

$$K \equiv \sqrt{4\pi}/a, \qquad X \equiv K/q, \qquad Z \equiv 2Kz = X\zeta. \tag{1.4}$$

1.2. Preview and summary

All our calculations start from the fields $\mathbf{E}$ and $\mathbf{B}$ quantized directly in terms of exact eigenmodes, as in section 2.2 of B.V. Except in section 4, potentials are neither needed nor used, whence the results are automatically (and trivially) gauge independent.

Section 2 writes down the operator f_z for the pressure experienced by the sheet; shows that it would vanish but for the odd-parity modes; shows that $\langle f_z^2 \rangle$ is nonzero even though $\langle f_z \rangle$ is; indicates (without evaluating it) the correlation function needed to determine the pressure fluctuations generally; and writes down the tangential (shear) stress operator $\mathbf{f}_\parallel$. In the nonretarded limit $c \to \infty$, the operator f_z vanishes but $\mathbf{f}_\parallel$ survives.

Section 3 determines $\langle \mathbf{E}^2 \rangle$ and $\langle \mathbf{B}^2 \rangle$, which emerge as functions of the scaled variable ζ. Section 3.2 finds the contribution from TE modes. Section 3.3 finds the *total* contribution from TM modes, including both TM photons and surface modes. This is a common strategy in such problems: it yields the end result as that part of a photon-derived contour integral that encircles just the branch cut of its integrand, to the exclusion of the residue from a pole, which is cancelled identically by the contribution from the surface modes. Section 3.4 looks at the general pattern of the results, best appreciated by concentrating on their asymptotics. The expressions for large enough ζ are of course the same in the realistically approachable limit where $z \to \infty$ at fixed q, and in the fanciful perfect-reflector (PR) limit as $q \to \infty$ at fixed z (see also appendix F). These asymptotic results, outside our thin sheet, coincide with the traditional ones that apply, in either of the corresponding limits, outside a half-space[1]. The

[1] For perfect reflectors, Bordag (2004) suggests that, on the contrary, the traditional expression (1.3) for $V_{\rm CP}$ applies only outside half-spaces, and fails outside thin enough sheets. His reasoning starts with the behaviour of E_z as $z \to 0$, but appears to turn, eventually, on choices of gauge. The present writer is unconvinced by the arguments about E_z, and (obviously) disagrees with the conclusions: the PR limit of our model yields (1.3) in a manifestly gauge-invariant way, for a thin sheet of precisely the kind for which Bordag claims a different result (smaller by a factor 13/15). He differs also about the first term on the right of our equation (4.2). Appendix F.2 below may have some bearing on these disagreements, which this is clearly not the place to pursue in detail.

agreement is interesting because for half-spaces (outside one or between two) experiments have verified $\langle \mathbf{E}^2 \rangle$, effectively through $V_{\rm CP}$, to an accuracy of roughly 10% (see Sukenik *et al* (1993), commented by Maddox (1993); the review by Hinds (1994); Sandoghdar *et al* (1996); Landragin *et al* (1996)).

Section 4 considers the interaction between the sheet and a slow charged particle, determining the part that is independent of Planck's constant. This part consists of the familiar image potential for a perfect reflector (irrespective of the value of q), plus another term Δ proportional to the squared components of the particle momentum. This calculation does require one to chose a gauge, and we use the pseudo-Coulomb gauge where $\boldsymbol{\nabla} \cdot \mathbf{A}$ vanishes except on the sheet. The result for Δ is a function only of ζ; hence it too yields one and the same expression as z, or q, or both, tend to infinity. Surprisingly perhaps, this indifference to the order of the limits appears to depend on dispersion: for a nondispersive dielectric half-space, Eberlein and Robaschik (2004) obtain different results depending on whether the large-distance limit or the perfect-reflector limit is taken first.

Appendices A and B deal with mathematical technicalities. The other appendices study consequences of possibly interesting but decidedly artificial restrictions or limits imposed on the physics of the model.

Appendix C considers the contributions $\langle \mathbf{E}^2 \rangle_{sp}$, $\langle \mathbf{B}^2 \rangle_{sp}$, and the corresponding u_{sp} just from the surface modes. Since they are given by single rather than by double integrals (over k but with no independent surface-normal wavenumber), they are easy to evaluate even under a cutoff. They are worth a glance because B.V has shown that (a) they require no Born subtractions, while (b) they dominate β. Thus U_{sp} dominates that part of β that resides off the sheet (namely the field energy, as opposed to the kinetic energy of the fluid). We show that U_{sp} is localized essentially within distances of order a from the sheet; which might be construed as a plausibility argument that the same is true for the Born-subtracted field energy even including the contributions from the photon modes. Appendix D determines u_{NR} and the localization of U_{NR} in the nonretarded model (B.V, appendix B), where surface plasmons are the only excitations.

Appendix E addresses effects that a cutoff would have on the unsubtracted mean-square fields. A complete calculation would be intolerably tedious, and the physics of the answers would be dubious anyway; hence we settle for just two conclusions. First, when $Z \gg 1$, corrections to the results from section 3 are of relative order $\exp(-Z)$, i.e. exponentially small. Second, as $z \to 0$ one finds that $\langle \mathbf{E}^2 \rangle$ and $\langle \mathbf{B}^2 \rangle$ continue to diverge even under the cutoff, with equal and opposite leading terms proportional respectively, to $\pm\hbar c q^4 X^2/2\pi\zeta$. Only u remains finite, its leading term the same as the nonretarded surface-mode contribution found in appendix D.

The last appendix, F, is concerned with $\langle \mathbf{E}^2 \rangle$ and $\langle \mathbf{B}^2 \rangle$ near a perfectly reflecting sheet. As explained in B.V, the problems raised by perfect reflection are largely artificial: we attend to them not for approximations to realizable physical systems, but because of their many links to the traditional literature on Casimir effects, and because they are responsible for misconceptions long past their sell-by date. Appendices F.1.1 and F.1.2 consider reflectors taken as perfect from the outset, without and with cutoff, respectively. Appendix F.2 then considers perfect reflection approached as a limit. The limit is shown to turn the flanking regions, $z \lessgtr 0$, into electromagnetically and quantally disjoint systems, each with its own Hilbert space, so that the overall Hilbert space reduces to the direct product of the mutually commuting Hilbert spaces for the two regions. The demonstration resolves a paradox by showing how this happens even though the odd-parity modes remain unaffected by the limit, as they do because they know nothing about the reflectivity.

2. Stresses

The pressure on the sheet (normal force per unit area) may be written as a sum of electric and magnetic contributions, $f_z = f_{ez} + f_{mz}$. Evidently

$$f_{ez} = \bar{E}_z \sigma = \bar{E}_z \frac{1}{4\pi} \,\mathrm{discont}(E_z), \qquad \bar{E}_z \equiv \frac{1}{2}\left[E_z(z=0+) + E_z(z=0-)\right], \tag{2.1}$$

where we have used Gauss's law. But $\bar{E}_z$ is nonzero only in odd-parity TM modes, and σ only in even-parity TM. Moreover, in these modes $\mathrm{discont}(E_z) = 2E_z(0+)$, and $\bar{E}_z = E_z(0+)$. Hence, in an obvious shorthand, and indicating also the magnetic pressure $f_{mz} = (\mathbf{J} \times \mathbf{B})_z$, one has

$$f_{ez} = \frac{1}{2\pi} E_z^{TM,-}\left(E_z^{TM,+} + E_z^{sp}\right), \qquad f_{mz} = \frac{1}{2\pi} \mathbf{B}_\parallel^{TM,-} \cdot \left(\mathbf{B}_\parallel^{TM,+} + \mathbf{B}_\parallel^{sp}\right), \qquad (z = 0+). \tag{2.2}$$

The same expressions follow from the Maxwell stress tensor.

It is worth emphasizing that the pressure operator would vanish but for the odd-parity modes, for all that they appear to be unaffected by the sheet. Thus the operator vanishes identically in the NR model, where there are only surface modes (which are pure even-parity TM). One can see this more directly from the fact that in the NR model the only forces are Coulomb forces between charges confined to the sheet, which interact only tangentially.

For the special case of perfect reflection the pattern (odd modes) $\times$ (even modes) can be foreseen directly from appendix F. Equation (F.12) there shows that, in an obvious shorthand for the normal modes,

$$(-) \times (+) \sim (R - L) \times (R + L) \sim (R^2 - L^2), \tag{2.3}$$

conformably to the sheet experiencing mutually independent (commuting) pressures on its two faces.

The ground-state expectation values of both pressure operators vanish by symmetry; but the pressure fluctuations do not vanish. To see this, we must first recall[2] (Barton 1991a, 1991b) that what is observable is not $f_z(t, \mathbf{s})$ itself, but only some average

$$\tilde{f}_z \equiv \int \mathrm{d}t \int \mathrm{d}^2 s \; g(t, T) h(\mathbf{s}, A) f_z(t, \mathbf{s}), \tag{2.4}$$

where g and h are apparatus-dependent sampling functions over some finite time interval of order T, and over some finite area of order A. Thus the measurable fluctuations read

$$\langle \tilde{f}_{ez}^2 \rangle = \frac{1}{4\pi^2} \langle \widetilde{\left(E_z^{TM,-}\right)^2} \rangle \left\{ \langle \widetilde{\left(E_z^{TM,+}\right)^2} \rangle + \langle \widetilde{\left(E_z^{sp}\right)^2} \rangle \right\} \neq 0. \tag{2.5}$$

It is easily verified that similar expectation values constructed from unaveraged squared fields would be divergent, i.e. ill-defined. The underlying quantity is the correlation function $\langle \{ f_z(t, \mathbf{s}),\, f_z(t', \mathbf{s}') \}_+ \rangle$; for perfect reflectors it is obtainable from its analogue for a half-space (Barton 1991b). For our plasma sheet it remains to be determined. In virtue of the fluctuation-dissipation theorem, it features also in the theory of the radiative reaction experienced by our plasma sheet when forced into nonuniform motion.

[2] Our present notation differs from these references, which would have written the average $\tilde{f}_z$ as $\widetilde{f}_z$, and the weighting functions g, h as f, ϕ, respectively. It is of the essence that $\tilde{f}_z$ is an average of f_z, which is bilinear in the fields, rather than a bilinear constructed from fields averaged beforehand. In (2.5), the typography may have stopped the tildes from extending right over the *squared* field components, as (2.4) shows that they should.

Analogous reasoning yields the shear stress (tangential force per unit area), whose electric and magnetic parts[3] read

$$\mathbf{f}_{e\parallel} = \bar{\mathbf{E}}_\parallel \sigma = \frac{1}{2\pi}\left(E_z^{TM,+} + E_z^{sp}\right)\left(\mathbf{E}_\parallel^{TM,+} + \mathbf{E}_\parallel^{sp}\right), \qquad (z = 0+), \tag{2.6}$$

$$\mathbf{f}_{m\parallel} = (\mathbf{J}\times\mathbf{B})_\parallel = \frac{1}{2\pi} B_z^{TE,+}\left(\mathbf{B}_\parallel^{TM,+} + \mathbf{B}_\parallel^{sp}\right), \qquad (z = 0+). \tag{2.7}$$

Here the odd modes play no role, and $\mathbf{f}_\parallel$ remains nonzero even in the NR model. In contrast, it vanishes for perfect reflectors (appendix E), in virtue of the boundary conditions $\mathbf{E}_\parallel = 0 = B_z$.

3. $\langle \mathbf{E}^2 \rangle$ and $\langle \mathbf{B}^2 \rangle$

3.1. Preliminaries

We study the total mean-squared fields, which we recall from section 1 are measurable in principle, and not now subject to Born subtractions. In particular, the odd-parity modes now contribute comparably with the even. Thus, though one might from curiosity consider the energy density u and its integral U from (1.2), the integral is not very interesting, and there is no reason why it should converge. In fact, without a cutoff (as in this section), U would diverge at its lower limit, while appendix E finds that with a cutoff U is finite.

Evidently one must calculate separately the contributions of the exact normal modes, TE and TM, even though for some purposes a subdivision according to $\parallel$ and $\perp$ field components might be preferable. The method is illustrated by sketching the calculation of $\langle \mathbf{E}^2 \rangle$, with $\langle \mathbf{B}^2 \rangle$ merely quoted.

3.2. TE modes

The field expansions in B.V yield

$$\langle \mathbf{E}^2 \rangle_{TE} = 2\pi \int_0^\infty \mathrm{d}k\, k \int_0^\infty \mathrm{d}p \frac{\hbar\omega}{2\pi^2 k^2}\{k^2 \sin^2(pz) + k^2\cos^2(pz+\eta)\} - (\text{counterterm}), \tag{3.1}$$

where the first (second) term comes from modes with odd (even) parity. The counterterm is the corresponding quantity in the absence of the mirror, namely the component independent of z. Hence the expression we want is found by setting

$$\sin^2(pz) = \frac{1-\cos(2pz)}{2} \to -\frac{\cos(2pz)}{2}, \tag{3.2}$$

$$\cos^2(pz+\eta) = \frac{1+\cos(2pz+2\eta)}{2} \to \frac{\cos(2pz+2\eta)}{2}, \tag{3.3}$$

where the arrows implement *the vacuum subtraction* explained in section 1.1. Using

$$(\cos(2\eta), \sin(2\eta)) = \frac{((p^2-q^2), (-2qp))}{q^2+p^2} \tag{3.4}$$

[3] One expects also a mechanical contribution $\mathbf{f}_{\mathrm{mech}\parallel}$ from the kinetic energy of the fluid. In an ideal classical 2D gas, the pressure (force across unit length) is just the kinetic energy per unit area, entailing $\langle \mathbf{f}_{\mathrm{mech}\parallel} \rangle = -\nabla_\parallel \langle \kappa_{\mathrm{op}} \rangle$. The spherical shell requires only the expectation value $\langle \kappa_{\mathrm{op}} \rangle \equiv \kappa$, which turns out to be essential for complying with the principle of virtual work applied to changes of the radius, i.e. to deformations normal to the sheet (B.III; and Barton 2004b, referred to as B.IV, section 3.3). But it is unclear to the writer how the principle might be applied to the uniform expansion of a flat sheet in its own plane.

and changing to integration variables[4] $y = k/q$, $x = p/q$, one eventually finds

$$\langle \mathbf{E}^2 \rangle_{TE} = \frac{\hbar c q^4}{\zeta^4} \mathcal{J}_E^{TE}(\zeta), \tag{3.5}$$

featuring the dimensionless form factor

$$\mathcal{J}_E^{TE}(\zeta) \equiv \frac{\zeta^4}{\pi} \int_0^\infty \mathrm{d}y\, y \int_0^\infty \mathrm{d}x \frac{\sqrt{x^2+y^2}}{x^2+1} \left\{ -\cos(\zeta x) + x \sin(\zeta x) \right\}. \tag{3.6}$$

The factors $\zeta^{\pm 4}$ prove convenient later. Note that $q^4/\zeta^4 = 1/16z^4$.

We choose $\zeta > 0$, and in hindsight start[5] by rearranging the integral over x. Write $\int_0^\infty \mathrm{d}x \ldots = (1/2) \int_{-\infty}^\infty \mathrm{d}x \ldots$, set

$$\frac{\{-\cos(\zeta x) + x \sin(\zeta x)\}}{x^2+1} = -\mathrm{Re}\left\{ \mathrm{i} \frac{\exp(\mathrm{i}\zeta x)}{x+\mathrm{i}} \right\}, \tag{3.7}$$

and displace the integration contour into the upper half of the complex x-plane, where the integrand has a branch cut from $\mathrm{i}y$ to $\mathrm{i}\infty$, but no poles. The new contour runs down just to the left of the cut, and up again just to the right. Then

$$\mathcal{J}_E^{TE} = \frac{\zeta^4}{\pi} \int_0^\infty \mathrm{d}y\, y \int_y^\infty \mathrm{d}x \exp(-\zeta x) \frac{\sqrt{x^2-y^2}}{x+1}. \tag{3.8}$$

Observing that $\int_0^\infty \mathrm{d}y y \int_y^\infty \mathrm{d}x \ldots = \int_0^\infty \mathrm{d}x \int_0^x \mathrm{d}y y \ldots$, we now integrate over y:

$$\begin{aligned} \mathcal{J}_E^{TE}(\zeta) &= \frac{\zeta^4}{3\pi} \int_0^\infty \mathrm{d}x \exp(-\zeta x) \frac{x^3}{x+1} \\ &= -\frac{\zeta^4}{3\pi} \frac{\partial^3}{\partial \zeta^3} \int_0^\infty \mathrm{d}x \frac{\exp(-\zeta x)}{x+1} = -\frac{\zeta^4}{3\pi} \frac{\partial^3}{\partial \zeta^3} \left\{ \exp(\zeta) E_1(\zeta) \right\}, \end{aligned} \tag{3.9}$$

$$\mathcal{J}_E^{TE}(\zeta) = \frac{1}{3\pi} \{ -\zeta^4 \exp(\zeta) E_1(\zeta) + \zeta^3 - \zeta^2 + 2\zeta \}, \tag{3.10}$$

where $E_1(\zeta) = \int_\zeta^\infty \mathrm{d}t \exp(-t)/t$ is the exponential integral. Asymptotically

$$\mathcal{J}_E^{TE}(\zeta \to \infty) = \frac{1}{\pi} \left\{ 2 - \frac{8}{\zeta} + \frac{40}{\zeta^2} - \frac{240}{\zeta^3} + \cdots \right\}, \tag{3.11}$$

$$\mathcal{J}_E^{TE}(\zeta \to 0) = \frac{1}{\pi} \left\{ \frac{2}{3}\zeta - \frac{1}{3}\zeta^2 + \frac{1}{3}\zeta^3 + \frac{1}{3}\left[\gamma + \log(\zeta) \right] \zeta^4 \ldots \right\}, \tag{3.12}$$

where $\gamma \simeq 0.5772$ is Euler's constant.

Similarly one finds

$$\langle \mathbf{B}^2 \rangle_{TE} = \frac{\hbar c q^4}{\zeta^4} \mathcal{J}_B^{TE}(\zeta), \qquad \mathcal{J}_B^{TE}(\zeta) = -5 \mathcal{J}_E^{TE}(\zeta). \tag{3.13}$$

The ratio -5 (regardless of ζ) is the same as for perfect reflectors (see appendix F).

[4] There will be no occasion to confuse these new scaled variables with the Cartesian coordinates in the plane of the sheet.

[5] Appendix A shows that the same result follows if one starts by integrating over y.

3.3. TM plus surface modes

Proceeding as for the TE modes, one is led straightforwardly to

$$\langle \mathbf{E}^2 \rangle_{TM} = 2\pi \int_0^\infty \mathrm{d}k\, k \int_0^\infty \mathrm{d}p \frac{\hbar\omega}{2\pi^2 k^2} \left(\frac{ck}{\omega}\right)^2 \{[k^2 \cos^2(pz) + p^2 \sin^2(pz)] + [k^2 \sin^2(pz+\mu) + p^2 \cos^2(pz+\mu)]\} - (\text{counterterm}), \tag{3.14}$$

$$\langle \mathbf{E}^2 \rangle_{TM} = \frac{\hbar c q^4}{\zeta^4} \mathcal{J}_E^{TM}(\zeta), \tag{3.15}$$

$$\mathcal{J}_E^{TM} = \frac{\zeta^4}{\pi} \int_0^\infty \mathrm{d}y\, y \int_0^\infty \mathrm{d}x \frac{y^2 - x^2}{\sqrt{x^2+y^2}} \frac{\{x^2 \cos(\zeta x) - x(x^2+y^2)\sin(\zeta x)\}}{[(x^2+y^2)^2 + x^2]}. \tag{3.16}$$

But from this point on the mathematics differ very significantly, reflecting the physical difference that the sp modes behave like bound states in the TM channel, whereas the TE channel has none.

Now, on preparing to evaluate $\int \mathrm{d}x \ldots$ in (3.16) by contour integration, $\mathcal{J}_E^{TM}$ becomes

$$\mathcal{J}_E^{TM} = \frac{\zeta^4}{\pi} \mathrm{Re} \int_0^\infty \mathrm{d}y y \frac{1}{2} \int_{-\infty}^\infty \mathrm{d}x \frac{y^2 - x^2}{\sqrt{x^2+y^2}} \frac{\mathrm{i}x \exp(\mathrm{i}\zeta x)}{[x^2 + \mathrm{i}x + y^2]}. \tag{3.17}$$

In the upper-half complex x-plane, the integrand has the same branch cut as one had for TE, but it also has a pole at

$$x = \mathrm{i}y_1, \qquad y_1 = (-1 + \sqrt{4y^2+1})/2 = \tilde{p}(k = qy)/q < y. \tag{3.18}$$

Accordingly

$$\langle \mathbf{E}^2 \rangle_{TM} = \langle \mathbf{E}^2 \rangle_{TM,\mathrm{pole}} + \langle \mathbf{E}^2 \rangle_{TM,\mathrm{cut}}.$$

It turns out that

$$\langle \mathbf{E}^2 \rangle_{TM,\mathrm{pole}} = -\langle \mathbf{E}^2 \rangle_{sp} :$$

in other words the contribution to $\langle \mathbf{E}^2 \rangle_{TM}$ from the pole identically cancels the contribution from the surface modes[6]. This is easy to verify either directly, or from equation (C.4) in the no-cutoff limit $Z_1 \to \infty$ given by (C.5). Hence we define the *total* TM contribution as

$$\langle \mathbf{E}^2 \rangle_{TMt} \equiv \langle \mathbf{E}^2 \rangle_{TM} + \langle \mathbf{E}^2 \rangle_{sp} = \langle \mathbf{E}^2 \rangle_{TM,\mathrm{cut}} \equiv \frac{\hbar c q^4}{\zeta^4} \mathcal{J}_E^{TMt}.$$

Thus

$$\langle \mathbf{E}^2 \rangle = \langle \mathbf{E}^2 \rangle_{TE} + \langle \mathbf{E}^2 \rangle_{TMt} \equiv \frac{\hbar c q^4}{\zeta^4} \mathcal{J}_E, \qquad \mathcal{J}_E = \mathcal{J}_E^{TE} + \mathcal{J}_E^{TMt}, \tag{3.19}$$

and we need pursue only[7] $\mathcal{J}_E^{TMt}$. Readily enough one finds

[6] This is a special case of perfectly general identities that operate in just the same way outside any dispersive mirror, for any $\langle F_i^2 \rangle$, and for many other related quantities. One important example is the level shift of an atom near a half-space of plasma, worked through by Babiker and Barton (1976). The cancellation operates separately for each value of y, i.e. for any given surface-parallel wavevector $\mathbf{k}$; hence it operates in the same way with as without a cutoff.

[7] Fortunately so, because to evaluate the $\mathcal{J}^{TM}$ directly one would have to integrate, very laboriously, along the real x-axis.

$$\mathcal{J}_E^{TMt} = \zeta^4 \int_0^\infty \mathrm{d}y\, y \int_y^\infty \mathrm{d}x \exp(-\zeta x) x \frac{y^2 + x^2}{\sqrt{x^2 - y^2}} \frac{1}{[x^2 + x - y^2]} \tag{3.20}$$

$$= \zeta^4 \int_0^\infty \mathrm{d}x \exp(-\zeta x) x \int_0^x \mathrm{d}y\, y \frac{y^2 + x^2}{\sqrt{x^2 - y^2}} \frac{1}{[x^2 + x - y^2]} \tag{3.21}$$

$$= \frac{\zeta^4}{\pi} \int_0^\infty \mathrm{d}x \exp(-\zeta x) \{-x^2 + 2x^{5/2} \tan^{-1}(x^{1/2}) + x^{3/2} \tan^{-1}(x^{1/2})\}, \tag{3.22}$$

having reversed the order of integration because the y integral in (3.21) is relatively easy whereas the x integral in (3.20) would prove very awkward. We write the result as

$$\mathcal{J}_E^{TMt} = \frac{\zeta^4}{\pi} \left\{ -\left[\frac{2}{\zeta^3} + A'(\zeta) \right] + 2A''(\zeta) \right\}, \tag{3.23}$$

in terms of the auxiliary function

$$A(\zeta) \equiv \int_0^\infty \mathrm{d}x \exp(-\zeta x) x^{1/2} \tan^{-1}(x^{1/2}) = -2 \frac{\partial}{\partial \zeta} \int_0^\infty \mathrm{d}x \exp(-\zeta x) \tan^{-1}(x^{1/2}) \tag{3.24}$$

which is analysed in appendix B.

For **B** we merely quote the analogues of the initial (3.14) and of the final (3.22) for **E**:

$$\langle \mathbf{B}^2 \rangle_{TM} = 2\pi \int_0^\infty \mathrm{d}k\, k \int_0^\infty \mathrm{d}p \frac{\hbar\omega}{2\pi^2 k^2} \{k^2 \cos^2(pz) + k^2 \sin^2(pz + \mu)\} - (\text{counterterm}), \tag{3.25}$$

$$\langle \mathbf{B}^2 \rangle_{TMt} = \frac{\hbar c q^4}{\zeta^4} \mathcal{J}_B^{TMt}(\zeta), \qquad \mathcal{J}_B^{TMt}(\zeta) = \frac{\zeta^4}{\pi} \left\{ -\frac{2}{\zeta^3} - A'(\zeta) \right\}. \tag{3.26}$$

Note that the component $[2/\zeta^3 + A'(\zeta)]$ is common to $\mathcal{J}_E^{TMt}$ and to $\mathcal{J}_B^{TMt}$.

The asymptotic approximations are constructed with A' and A'' from appendix B, and turn out to read

$$\mathcal{J}_E^{TMt}(\zeta \to \infty) = \frac{1}{\pi} \left\{ 10 - \frac{56}{5\zeta} + \frac{216}{7\zeta^2} - \frac{880}{7\zeta^3} + \cdots \right\}, \tag{3.27}$$

$$\mathcal{J}_B^{TMt}(\zeta \to \infty) = \frac{1}{\pi} \left\{ -2 + \frac{24}{5\zeta} - \frac{120}{7\zeta^2} + \frac{80}{\zeta^3} + \cdots \right\}; \tag{3.28}$$

$$\mathcal{J}_E^{TMt}(\zeta \to 0) = \frac{1}{\pi} \left\{ \frac{15\pi^{3/2}\zeta^{1/2}}{8} - 6\zeta + \frac{3\pi^{3/2}\zeta^{3/2}}{8} - \frac{\zeta^2}{3} - \frac{\zeta^3}{15} + \left[\frac{2}{1225} - \frac{3}{35} (\gamma + \log(\zeta)) \right] \zeta^4 + \cdots \right\}, \tag{3.29}$$

$$\mathcal{J}_B^{TMt}(\zeta \to 0) = \frac{1}{\pi} \left\{ -2\zeta + \frac{3\pi^{3/2}\zeta^{3/2}}{8} - \zeta^2 + \frac{\zeta^3}{3} + \left[-\frac{2}{25} + \frac{1}{5} (\gamma + \log(\zeta)) \right] \zeta^4 + \cdots . \right\}. \tag{3.30}$$

The results for small ζ have been given to $\mathcal{O}(\zeta^4)$, in order to identify those parts of the mean-square fields that remain finite as $\zeta \to 0$.

3.4. General patterns and asymptotics

We define

$$\mathcal{J}_E = \mathcal{J}_E^{TE} + \mathcal{J}_E^{TMt}, \qquad \mathcal{J}_B = \mathcal{J}_B^{TE} + \mathcal{J}_B^{TMt}, \qquad \mathcal{J}_u \equiv \mathcal{J}_E + \mathcal{J}_B, \tag{3.31}$$

where the suffix on $\mathcal{J}_u$ alludes to the energy density u from (1.2), but without the factor $1/8\pi$.

Asymptotically (though in fact the series for low ζ converge):

$$\mathcal{J}_E(\zeta \to \infty) = \frac{1}{\pi}\left\{12 - \frac{96}{5\zeta} + \frac{496}{7\zeta^2} - \frac{2560}{7\zeta^3} + \cdots\right\}, \tag{3.32}$$

$$\mathcal{J}_B(\zeta \to \infty) = \frac{1}{\pi}\left\{-12 + \frac{224}{5\zeta} - \frac{1520}{7\zeta^2} + \frac{1280}{\zeta^3} + \cdots\right\}, \tag{3.33}$$

$$\mathcal{J}_u(\zeta \to \infty) = \frac{1}{\pi}\left\{\frac{128}{5\zeta} - \frac{1024}{7\zeta^2} + \frac{6400}{7\zeta^3} + \cdots\right\}; \tag{3.34}$$

$$\mathcal{J}_E(\zeta \to 0) = \frac{1}{\pi}\left\{\frac{15\pi^{3/2}\zeta^{1/2}}{8} - \frac{16\zeta}{3} + \frac{3\pi^{3/2}\zeta^{3/2}}{8} - \frac{2\zeta^2}{3} + \frac{4\zeta^3}{15} + \left[\frac{2}{1225} + \frac{26}{105}\left(\gamma + \log(\zeta)\right)\right]\zeta^4 + \cdots\right\}, \tag{3.35}$$

$$\mathcal{J}_B(\zeta \to 0) = \frac{1}{\pi}\left\{-\frac{16\zeta}{3} + \frac{3\pi^{3/2}\zeta^{3/2}}{8} + \frac{2\zeta^2}{3} - \frac{4\zeta^3}{3} - \left[\frac{2}{25} + \frac{22}{15}\left(\gamma + \log(\zeta)\right)\right]\zeta^4 + \cdots\right\}, \tag{3.36}$$

$$\mathcal{J}_u(\zeta \to 0) = \frac{1}{\pi}\left\{\left[\frac{15\pi^{3/2}\zeta^{1/2}}{8} + \frac{3\pi^{3/2}\zeta^{3/2}}{4}\right] - \frac{32\zeta}{3} - \frac{16\zeta^3}{15} - \left[\frac{96}{1225} + \frac{128}{105}\left(\gamma + \log(\zeta)\right)\right]\zeta^4 + \cdots\right\}. \tag{3.37}$$

For comparison, we anticipate from section 4 the surface-plasmon contribution without cutoff (which, via $\mathcal{J}^{TMt}$, is already included in the $\mathcal{J}_{E,B}$). One finds

$$\mathcal{J}_E^{sp} = \frac{15\pi^{3/2}\zeta^{1/2}}{8} + \frac{3\pi^{3/2}\zeta^{3/2}}{8}, \qquad \mathcal{J}_B^{sp} = \frac{3\pi^{3/2}\zeta^{3/2}}{8}, \tag{3.38}$$

$$\mathcal{J}_u \equiv \mathcal{J}_E^{sp} + \mathcal{J}_B^{sp} = \frac{15\pi^{3/2}\zeta^{1/2}}{8} + \frac{3\pi^{3/2}\zeta^{3/2}}{4}. \tag{3.39}$$

Thus, at high ζ the surface modes by themselves yield no clues at all to the true results; but at low ζ they supply the entire leading term of $\mathcal{J}_E$ and thereby of $\mathcal{J}_u$. In fact they then supply both the terms with fractional powers of ζ.

Note also that, as $\zeta \to \infty$, the leading terms of $\mathcal{J}_{E,B}^{TE}, \mathcal{J}_{E,B}^{TMt}$ tally with the perfect-reflector limits from appendix F, cancelling in the same way, so that $\mathcal{J}_u$ is of order $1/\zeta$, and $u \simeq \hbar c/10\pi^2 q z^5$. Accordingly, figure 1 plots $(\pi/12)J_E$ and $-(\pi/12)\mathcal{J}_B$, which approach their perfect-reflector value of 1 as $\zeta \to \infty$; and also the combination $(\pi/12)(\mathcal{J}_E + \mathcal{J}_B)$, which vanishes as $\zeta \to \infty$, and for perfect reflectors would vanish everywhere.

Finally, reverting to u and U, equation (1.2), we can now verify what section 3.1 claimed about integrability, and note also that $u(z)$ is always positive (which appendix E shows it to remain even under a cutoff). Though from our present point of view the sign of u is secondary, it is sometimes studied on account of wider field-theoretic implications that negative energy

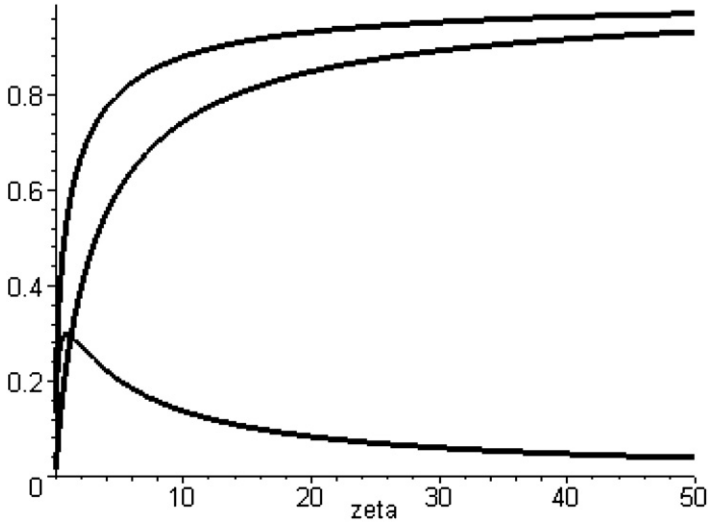

Figure 1. The form factors for the mean-square fields without cutoff, as functions of ζ. Top curve: $(\pi/12)\mathcal{J}_E$; middle curve: $-(\pi/12)\mathcal{J}_B$. These curves approach +1 as $\zeta \to \infty$. Bottom curve: $(\pi/12)\mathcal{J}_f$, where $\mathcal{J}_f \equiv \mathcal{J}_E + \mathcal{J}_B$. This combination vanishes for perfect reflection. The asymptotics are given by equations (3.32)–(3.34) as $\zeta \to \infty$, and by (3.35)–(3.37) as $\zeta \to 0$.

densities might have if they extended over appreciable regions of space. In particular, u has been shown to be positive by Helfer and Lang (1999) everywhere outside a nondispersive half-space; by Sopova and Ford (2002) everywhere outside a plasma half-space; and by Graham, Olum and Schwartz-Perlov (2004) everywhere outside a solid nondispersive sphere. Our own results extend these conclusions to our very simple model of a flat dispersive mirror; and it seems likely that they could be extended also to the dispersive spherical shells considered in B.III and B.IV.

4. The classical interaction between the sheet and a charged particle

Unlike all else in this paper, the interaction of the sheet with a charged point particle, at a distance z and having charge Q, mass M and momentum $\mathbf{P}$, will be derived only perturbatively, and requires a Hamiltonian in canonical form, which in turn requires commitment to some definite gauge. We choose the pseudo-Coulomb gauge (Barton 1977), which expresses our quantized fields as $\mathbf{E} = -\dot{\mathbf{A}}/c$, $\mathbf{B} = \boldsymbol{\nabla} \times \mathbf{A}$; then $\boldsymbol{\nabla} \cdot \mathbf{A}$ vanishes except on the sheet, and the interaction Hamiltonian reads

$$H_{\text{int}} = -Q^2/4\,|z| - Q\mathbf{A} \cdot \mathbf{P}/Mc + Q^2\mathbf{A}^2/2Mc^2. \tag{4.1}$$

The first term is the same as the classical image potential experienced by a stationary charge near a perfect mirror (regardless of how well the plasma actually reflects, i.e. regardless of q). For a slow particle, the pseudo-Coulomb gauge delivers the leading momentum-dependent corrections through the energy shift calculated in second-order perturbation theory from the middle term of H_{int}. These shifts, quadratic in $\mathbf{P}$, likewise turn out to be free of $\hbar$, i.e. purely classical[8]; for a perfect mirror they stem wholly from TE photons, and read

$$\Delta^{(\text{PR})} = (Q/Mc)^2\big(-P_z^2 + \mathbf{P}_\parallel^2/2\big)\big/4z. \tag{4.2}$$

[8] The leading quantal shift $(Q^2/2Mc^2)\langle\mathbf{A}^2\rangle$ is the kinetic energy forced on the particle by the zero-point oscillations of the quantized $\mathbf{E}$ field: see, e.g., Barton (1989), appendix. As $q \to \infty$ or as $|z| \to \infty$ it becomes $Q^2\hbar/4\pi Mc^2z^2$.

For brevity we define[9]

$$\Delta(\mathbf{P}) \equiv \left\{\Delta_z(z)P_z^2 + \Delta_\parallel(z)\mathbf{P}_\parallel^2\right\}. \tag{4.3}$$

The first component is understood as shorthand for $\left\{\Delta_z(z)P_z^2 + P_z^2\Delta_z(z)\right\}/2$: just how one chooses to symmetrize affects only the quantal components of the shift, proportional to higher powers of $1/z$. The aim here is to determine Δ for our model, in order to complete the classical part of the shift, and to illustrate how it adapts to dispersion. Besides, it is interesting to contrast the outcome with the conclusions of Eberlein and Robaschik (2004) for a nondispersive half-space, where they find different results when the perfect-reflector limit is taken at the start or at the end of the calculation. We shall see, in contrast, that in our dispersive model there are no such ambiguities: $\lim_{q\to\infty}\Delta$ reproduces (4.2) quite trivially.

We adopt the no-recoil approximation: from the perturbative energy denominators, this drops the change in the kinetic energy of the particle, and keeps only the energy of the virtual surface plasmon or photon. Its applicability is discussed elsewhere (Barton 1977).

The calculation requires the normal-mode amplitudes of $\mathbf{A}$, related to those of $\mathbf{E}$ through

$$\mathbf{A}_{\mathbf{k},p}^{(j)} = (-\mathrm{i}c/\omega)\mathbf{E}_{\mathbf{k},p}^{(j)}, \qquad \mathbf{A}_{\mathbf{k}}^{(sp)} = (-\mathrm{i}c/\Omega)\mathbf{E}_{\mathbf{k}}^{(sp)}. \tag{4.4}$$

The virtual-surface-plasmon contribution reads

$$\Delta_{sp} = -\left(\frac{Q}{Mc}\right)^2 2\pi\int_0^\infty \mathrm{d}k\, k\frac{1}{\hbar\Omega}\left(\frac{c}{\Omega}\right)^2 N_k^2\exp(-2\tilde{p}z)\left(\frac{ck}{\Omega}\right)^2\left\{P_z^2k^2 + \frac{1}{2}\mathbf{P}_\parallel^2\tilde{p}^2\right\},$$

where the factor $1/2$ stems from the integration of $(\hat{\mathbf{k}}\cdot\mathbf{P}_\parallel)^2$ over the polar angle of $\hat{\mathbf{k}}$. Planck's constant disappears because the factor $\hbar$ in N_k^2 cancels the factor $\hbar$ in the energy denominator $\hbar\Omega$; a similar mechanism operates in the photon contributions considered below. On changing the integration variable to $\tilde{p}$, straightforward manipulation eventually yields

$$\Delta_{sp} = -\left(\frac{Q}{Mc}\right)^2\left\{P_z^2\left[\frac{1}{4z} + \frac{1}{8qz^2}\right] + \frac{1}{2}\mathbf{P}_\parallel^2\frac{1}{8qz^2}\right\}. \tag{4.5}$$

There are virtual-photon contributions from modes of both parities. We make the replacements (3.2)–(3.4) etc, scale variables and find

$$\begin{aligned}\Delta_{TE} &= \left(\frac{Q}{Mc}\right)^2\frac{1}{2}\mathbf{P}_\parallel^2\frac{q}{\pi}\int_0^\infty \mathrm{d}y\, y\int_0^\infty \mathrm{d}x\frac{[\cos(\zeta x) - x\sin(\zeta x)]}{(x^2+y^2)(x^2+1)}\\ &= \left(\frac{Q}{Mc}\right)^2\frac{1}{2}\mathbf{P}_\parallel^2\frac{q}{4\pi}\int_0^\infty \mathrm{d}y\,\mathrm{Re}\int_{-\infty}^\infty \mathrm{d}x\frac{\exp(\mathrm{i}\zeta x)}{(x+\mathrm{i})}\left[\frac{1}{(x-\mathrm{i}y)} - \frac{1}{(x+\mathrm{i}y)}\right].\end{aligned}$$

Only the pole at $x = \mathrm{i}y$ contributes to the contour integral closed (when $\zeta > 0$) in the upper-half x plane:

$$\Delta_{TE} = \frac{1}{2}\mathbf{P}_\parallel^2\left(\frac{Q}{Mc}\right)^2\frac{q}{2}\int_0^\infty \mathrm{d}y\frac{\exp(-\zeta y)}{(y+1)} = \frac{1}{2}\mathbf{P}_\parallel^2\left(\frac{Q}{Mc}\right)^2\frac{q}{2}\exp(\zeta)E_1(\zeta). \tag{4.6}$$

Similarly but more laboriously one finds[10]

$$\begin{aligned}\Delta_{TM} = \left(\frac{Q}{Mc}\right)^2\frac{q}{2\pi}\int_0^\infty \mathrm{d}y\, y\ \mathrm{Re}\frac{1}{\mathrm{i}}\int_{-\infty}^\infty \frac{\mathrm{d}x\, x}{(x+\mathrm{i}y)^2(x-\mathrm{i}y)^2}\\ \times\frac{\exp(\mathrm{i}\zeta x)}{(x^2+y^2+\mathrm{i}x)}\left\{P_z^2y^2 - \frac{1}{2}\mathbf{P}_\parallel^2x^2\right\} = 0.\end{aligned} \tag{4.7}$$

[9] Thus the particle is governed by an effective Hamiltonian $H_{\mathrm{eff}} = P^2/2M - Q^2/4|z| + \Delta(\mathbf{P})$. In terms of the velocity $\mathbf{V} = \partial H_{\mathrm{eff}}/\partial\mathbf{P}$ this reads $H_{\mathrm{eff}} = M\mathbf{V}^2/2 - Q^2/4|z| - \Delta(M\mathbf{V})$. In other words the shift at fixed $\mathbf{V}$ is the negative of the shift at fixed $\mathbf{P}$.

[10] The last equality in (4.7) holds for all real nonzero ζ. However, though (trivially) $\lim_{\zeta\to0}\Delta_{TM} = 0$, the limit may not be taken under the integrals. If, in the integrand, one were to set $\exp(\mathrm{i}\zeta x) \to 0$ from the start, then (4.7) would yield finite and nonzero Δ_z and $\Delta_\parallel$, negative and positive, respectively.

It is remarkable that Δ_{TM} vanishes for all q (i.e. not only for perfect reflectors), and the writer can detect no advance warning of the fact directly from (4.7). There are two methods of showing it.

The first method is ad hoc: change to plane-polar integration variables r, θ defined by $(x, y) = r(\cos\theta, \sin\theta)$, with $0 \leqslant r < \infty$ and $0 \leqslant \theta \leqslant \pi$; integrate over r; and observe that the resulting function of θ is odd around the mid-point $\theta = \pi/2$.

The second method is generic, and perhaps more instructive. As for TE, the contour is closed in the upper-half x plane, yielding two contributions. One comes from the already familiar pole due to the zero of $(x^2 + y^2 + \mathrm{i}x)$ at $x = \mathrm{i}y_1$ (see (3.17), (3.18), and appendix C of B.V). As expected (see the first footnote in section 3.3), this equals $-\Delta_{sp}$. The other contribution comes from the double pole at $x = \mathrm{i}y$, and by a startling coincidence it eventually turns out to equal $+\Delta_{sp}$, so that

$$\Delta_{TM} = \Delta_{TM,\text{pole}} + \Delta_{TM,\text{double pole}} = -\Delta_{sp} + \Delta_{sp} = 0 \tag{4.8}$$

does indeed vanish. In other words, defining a *total* TM contribution (cf section 3.3) we find

$$\Delta_{TMt} \equiv \Delta_{TM} + \Delta_{sp} = 0 + \Delta_{sp} = \Delta_{sp}. \tag{4.9}$$

Thus the end result is

$$\Delta = \Delta_{TE} + \Delta_{sp} = \left(\frac{Q}{Mc}\right)^2 \left\{-P_z^2\left[\frac{1}{4z} + \frac{1}{8qz^2}\right] + \frac{1}{2}\mathbf{P}_\parallel^2\left[\frac{q}{2}e^\zeta E_1(\zeta) - \frac{1}{8qz^2}\right]\right\}. \tag{4.10}$$

For large ζ it yields

$$\Delta = \left(\frac{Q}{Mc}\right)^2 \left\{-P_z^2\left[\frac{1}{4z} + \frac{1}{8qz^2}\right] + \frac{1}{2}\mathbf{P}_\parallel^2\left[\frac{1}{4z} - \frac{1}{4qz^2} + \mathcal{O}\left(\frac{1}{q^2z^3}\right)\right]\right\}, \tag{4.11}$$

which in the limit $q \to \infty$ at fixed z reproduces (4.2), as promised.

Acknowledgments

It is a pleasure to thank Michael Bordag, Claudia Eberlein and Dieter Robaschik for stimulating comments on their papers.

Appendix A. The order of the integrations in $\mathcal{J}_E^{TE}$

We show that, for our purposes,

$$\int_0^\infty \mathrm{d}y\, y \int_0^\infty \frac{\mathrm{d}x}{x^2+1}\{-\cos(\zeta x) + x\sin(\zeta x)\}\sqrt{x^2+y^2} = \int_0^\infty \frac{\mathrm{d}x}{x^2+1}\{-\cos(\zeta x) + x\sin(\zeta x)\}\int_0^\infty \mathrm{d}y\, y\sqrt{x^2+y^2}. \tag{A.1}$$

Evaluating $\mathcal{J}_E^{TE}$ in section 3.2 we started with the left-hand expression, turned $\int_0^\infty \mathrm{d}x \ldots$ at fixed y into a far more convenient contour integral, performed $\int \mathrm{d}y \ldots$, and then $\int \mathrm{d}x \ldots$.

Now we start instead with the right-hand side of (A.1), and, *before* doing anything to the x-integrand, implement $\int \mathrm{d}y \ldots$, for all that it seems to diverge. The argument hinges on the fact that

$$\int_0^\infty \frac{\mathrm{d}x}{x^2+1}\{-\cos(\zeta x) + x\sin(\zeta x)\} = 0, \tag{A.2}$$

which allows us to drop from $\int \mathrm{d}y \ldots$ any parts that are independent of x, even if they are divergent. Thus we set

$$\int_0^\infty \mathrm{d}y\, y\sqrt{x^2+y^2} = \frac{1}{3}(x^2+y^2)^{3/2}\Big|_{y=0}^{\infty} = \infty - \frac{1}{3}x^3 \to -\frac{1}{3}x^3,$$

whence

$$\mathcal{J}_E^{TE} = -\frac{\zeta^4}{3\pi}\int_0^\infty \frac{\mathrm{d}x x^3}{x^2+1}\{-\cos(\zeta x) + x\sin(\zeta x)\} = -\frac{\zeta^4}{3\pi}\frac{\partial^3}{\partial\zeta^3}\left(1+\frac{\partial}{\partial\zeta}\right)\int_0^\infty \frac{\mathrm{d}x\sin(\zeta x)}{x^2+1}. \tag{A.3}$$

Finally, on rotating integration contours to the imaginary axis, the rightmost expression is seen to agree with (3.9), as claimed.

Appendix B. The function $A(\zeta)$

We study the function A defined by (3.24), mainly in order to establish a more flexible representation, and convenient expansions of

$$\{A, -A', A''\} = \int_0^\infty \mathrm{d}x \exp(-\zeta x)\tan^{-1}(x^{1/2})\{x^{1/2}, x^{3/2}x^{5/2}\} \tag{B.1}$$

at large and small ζ.

In fact, for large ζ one need only expand the arctangent for small values of its argument, and integrate term by term. This yields the divergent asymptotic series

$$A = \sum_{n=0}^{\infty}(-1)^n\frac{(n+1)!}{(2n+1)\zeta^{n+2}} = \frac{1}{\zeta^2} - \frac{2}{3\zeta^3} + \frac{6}{5\zeta^4} - \frac{24}{7\zeta^5} + \frac{40}{3\zeta^6} - \frac{720}{11\zeta^7} + \cdots, \tag{B.2}$$

and A', A'' by differentiation.

To go further, we start with the definition of A, change the integration variable to $y = \sqrt{x}$ and integrate by parts to obtain

$$\begin{aligned} A &= A_1 + A_2 + A_3, \\ A_1 &= \frac{4\zeta}{3}\int_0^\infty \mathrm{d}y\, y^4\tan^{-1}(y)\exp(-\zeta y^2) = -\frac{2\zeta}{3}A', \end{aligned} \tag{B.3}$$

where the last step follows on reverting from y to x;

$$\begin{aligned} A_2 &= -\frac{2\zeta}{3}\int_0^\infty \mathrm{d}y\, y^3\exp(-\zeta y^2) = -\frac{1}{3\zeta}; \\ A_3 &= \frac{\zeta}{3}\int_0^\infty \mathrm{d}x\exp(-\zeta x)\log(1+x) = \frac{1}{3}\exp(\zeta)E_1(\zeta), \end{aligned}$$

where again we have reverted to x and have integrated by parts. Substituting back into (B.3) and rearranging the result, we obtain a differential equation for A, namely

$$A' + \frac{3}{2\zeta}A = -\frac{1}{2\zeta^2} + \frac{1}{2\zeta}\exp(\zeta)E_1(\zeta). \tag{B.4}$$

Multiplying with the integrating factor $\zeta^{3/2}$, integrating from 0 to ζ and using the end-point condition

$$\lim_{\zeta\to 0}\zeta^{3/2}A = \lim_{\zeta\to 0}\zeta^{3/2}\int_0^\infty \mathrm{d}x\exp(-\zeta x)x^{1/2}\pi/2 = \pi^{3/2}/4, \tag{B.5}$$

one obtains

$$A(\zeta) = \frac{\pi^{3/2}}{4\zeta^{3/2}} - \frac{1}{\zeta} + \frac{1}{2\zeta^{3/2}} L(\zeta), \qquad L \equiv \int_0^\zeta \mathrm{d}t\, t^{1/2} \exp(t) E_1(t). \tag{B.6}$$

A convergent series for L and thereby for A, useful at low to moderate values of ζ, follows from

$$E_1(t) = -\gamma - \log(t) - \sum_{n=1}^{\infty} (-1)^n \frac{t^n}{n!n}. \tag{B.7}$$

Then one writes the integrand of L as a power series in $\sqrt{t}$ plus $\log(t)$ times another such series, and integrates term by term. The result for A starts as

$$A = \frac{\pi^{3/2}}{4\zeta^{3/2}} - \frac{1}{\zeta} + \frac{1}{3}\left[\frac{2}{3} - \gamma - \log(\zeta)\right] + \zeta \frac{1}{5}\left[\frac{7}{35} - \gamma - \log(\zeta)\right] + \zeta^2 \frac{1}{14}\left[\frac{25}{14} - \gamma - \log(\zeta)\right]$$
$$+ \zeta^3 \frac{1}{54}\left[\frac{37}{18} - \gamma - \log(\zeta)\right] + \zeta^4 \frac{1}{264}\left[\frac{299}{132} - \gamma - \log(\zeta)\right] + \cdots. \tag{B.8}$$

Series for A' and A'' follow by differentiation.

Appendix C. Surface modes: details

There are two main reasons for considering surface plasmons in somewhat more detail than photons.

(i) Their mean-squared fields can be found in closed form even under a cutoff. Loosely speaking these expressions illustrate the extreme opposite to perfect reflection, where appendix F likewise manages a cutoff in closed form, but where no surface modes are seen. However, we recall from section 1 that, as regards the fields, cutoffs can be taken only with a large grain of salt.

(ii) We know from B.V that the surface-mode contribution to the cohesive energy β is (a) dominant, and (b) not subject to Born subtractions (unlike that of photons). Thus, if[11] one is content to enquire into the localization only of β (which means disregarding self-energy contributions to the mean-square fields), then to leading order the question can be answered from a knowledge only of $u_{sp} \equiv (\langle \mathbf{E}^2 \rangle_{sp} + \langle \mathbf{B}^2 \rangle_{sp})/8\pi$.

To handle the cutoff, we recall from (1.4) the dimensionless parameters X and Z, and (cf B.V, sections 3.2 and 3.3.2) define also their relatives

$$X_1 \equiv \left\{\sqrt{4X^2 + 1} - 1\right\}/2, \qquad Z_1 \equiv X_1 \zeta = (X_1/X) Z. \tag{C.1}$$

Thus, for large X one has $X_1 \simeq X$:

$$X_1 = X - 1/2 + \mathcal{O}(1/X); \tag{C.2}$$

on the other hand, for small X,

$$X_1 = X^2 + \mathcal{O}(X^4). \tag{C.3}$$

[11] The *if* is less restrictive than one might have thought. Without the Born subtraction, the energy density u diverges nonintegrably as $z \to 0$, so that there is no well-defined total quantity whose distribution u could be said to describe.

C.1. The mean-square fields under cutoff

The mean-square fields follow directly from B.V, equations (2.23), (2.29), (2.30). We change the integration variable from k to $\tilde{p}$ to $\tilde{p}/q$, recall $Z_1 = Z \cdot (X_1/X)$, and find[12]

$$\begin{aligned}\begin{pmatrix}\langle \mathbf{E}^2\rangle_{sp}\\ \langle \mathbf{B}^2\rangle_{sp}\end{pmatrix} &= 2\pi \int_0^K \mathrm{d}k\, k N_k^2 \exp(-2\tilde{p}z) \begin{pmatrix}(ck/\Omega)^2(k^2+\tilde{p}^2)\\ k^2\end{pmatrix}\\ &= \hbar c q^4 \begin{pmatrix}\zeta^{-7/2}\mathcal{I}_1 + \zeta^{-5/2}\mathcal{I}_2/2\\ \zeta^{-5/2}\mathcal{I}_2/2\end{pmatrix},\end{aligned} \tag{C.4}$$

where

$$\begin{pmatrix}\mathcal{I}_1(Z_1)\\ \mathcal{I}_2(Z_1)\end{pmatrix} \equiv \int_0^{Z_1} \mathrm{d}y \exp(-y) \begin{pmatrix}y^{5/2}\\ y^{3/2}\end{pmatrix} \underset{Z_1\to\infty}{\to} \begin{pmatrix}(15\sqrt{\pi}/8)\\ (3\sqrt{\pi}/4)\end{pmatrix}. \tag{C.5}$$

Comparison with the *NR* model (appendix D) shows that $\mathcal{I}_1(\cdot) = \mathcal{I}_{NR}(\cdot)$.

The rightmost expression in (C.5) is approached in the no-cutoff limit ($K \to \infty$ at fixed z), and also at large distance ($z \to \infty$ at fixed K). Then there is little difference between (X_1, Z_1) and (X, Z). Under cutoff, the exact form factors are

$$\mathcal{I}_1(Z_1) = \frac{15\sqrt{\pi}}{8}\mathrm{erf}(\sqrt{Z_1}) - \mathrm{e}^{-Z_1}\left\{\frac{15}{4}Z_1^{1/2} + \frac{5}{2}Z_1^{3/2} + Z_1^{5/2}\right\} = \frac{15\sqrt{\pi}}{8} + \mathcal{O}\big(\mathrm{e}^{-Z_1}Z_1^{5/2}\big), \tag{C.6}$$

$$\mathcal{I}_2(Z_1) = \frac{3\sqrt{\pi}}{4}\mathrm{erf}(\sqrt{Z_1}) - \mathrm{e}^{-Z_1}\left\{\frac{3}{2}Z_1^{1/2} + Z_1^{3/2}\right\} = \frac{3\sqrt{\pi}}{4} + \mathcal{O}\big(\mathrm{e}^{-Z_1}Z_1^{3/2}\big). \tag{C.7}$$

In contrast, as $Z_1 \to 0$ equations (C.6), (C.7) entail

$$\mathcal{I}_1(Z_1) = \tfrac{2}{7}Z_1^{7/2} - \tfrac{2}{9}Z_1^{9/2} + \ldots, \qquad \mathcal{I}_2(Z_1) \equiv \tfrac{2}{5}Z_1^{5/2} - \tfrac{2}{7}Z_1^{7/2} + \cdots. \tag{C.8}$$

We consider only the realistic regime where $X \gg 1$. Then $\zeta^{-7/2}\mathcal{I}_1$ and therefore $\langle \mathbf{E}^2\rangle_{sp}$ evidently dominate for small Z_1, while $\zeta^{-5/2}\mathcal{I}_2$ dominates at large Z_1, making $\langle \mathbf{E}^2\rangle_{sp}$ and $\langle \mathbf{B}^2\rangle_{sp}$ comparable. The cross-over occurs where $\mathcal{I}_1(Z_1) = \zeta\mathcal{I}_2 = (Z_1/X_1)\mathcal{I}_2(Z_1)$, which happens at $Z_1/X_1 \sim O(1)$, so that $Z_1 \sim X_1 \gg 1$. But then the no-cutoff approximation (C.5) applies, whence $Z_1 \simeq 5X_1/2$ and $\zeta \simeq 5/2$. In other words the crossover happens at $z \sim 1/q \sim a^2/r_0 \gg a$.

C.2. The localization of the sp field energy

To appreciate how *sp* field energy is distributed in space, we scale it to β_{sp} (B.V, equation (3.6)); scale distance z to $1/2K = a/4\sqrt{\pi}$ (chosen by hindsight as a convenient alternative to a), so that the scaled distance becomes $2Kz = Z$; and write ρ_{sp} for the correspondingly scaled dimensionless density. Then

$$\rho_{sp} \equiv \frac{u_{sp}}{2K\beta_{sp}} = \frac{5}{16\pi}\frac{[\mathcal{I}_1(Z_1) + Z_1\mathcal{I}_2(Z_1)/X_1]}{Z_1^{7/2}[1 + 5/3X_1]}. \tag{C.9}$$

The crucial point is that this is a function of z only through $Z_1 = Z(X_1/X)$, i.e. only through Z. *Therefore u_{sp} is concentrated within distances from the sheet of order $1/K \sim a$.*

[12] For photon modes, section 3 introduced form factors $\mathcal{J}$ such that, for instance, $\langle \mathbf{E}^2\rangle_{TE} = \big(\hbar c q^4/\zeta^4\big)\mathcal{J}_E^{TE}(\zeta)$, a definition constructed so that $\mathcal{J}_E^{TE}(\infty)$ is a finite constant determined by the perfect-reflector limit (appendix F). This is not a natural normalization for *sp* contributions, which behave differently at large z; but for purposes of comparison we note that the correspondingly normed *sp* form factors would be related to $\mathcal{I}_{1,2}$ by $\mathcal{J}_1^{sp} = \zeta^{1/2}\mathcal{I}_1$ and $\mathcal{J}_2^{sp} = \zeta^{3/2}\mathcal{I}_2$.

The analogous demonstration for the NR model is even simpler, and follows on dimensional grounds alone, as in appendix D below. In contrast, retarded u, having the extra input parameter c, can contain contributions proportional to $\hbar c/z^4$, as the archetypal perfect-reflector limits of the mean-square fields famously do. Hence for u_{sp} dimensional argument fail, and only explicit calculation can serve.

C.3. Excitation of surface modes

Since surface plasmons cannot be excited by photons, it is instructive to calculate the rate Γ_{sp} of their emission by an excited atom a distance z from the sheet. (We do not pursue here the classic problem of how the sheet affects the emission rates of photons.)

For z much greater than the atomic radius, one can use the dipole approximation to the interaction Hamiltonian, writing it as

$$H_{\rm int} = -\mathbf{D}\cdot\mathbf{E}, \tag{C.10}$$

where $\mathbf{D}$ is the atomic dipole-moment operator, with matrix elements $\mathbf{D}_{fi}$ between the initial and final atomic states i and f. The Golden Rule of time-dependent perturbation theory and the expansion of $\mathbf{E}$ (equations (2.23), (2.29), (2.30) in B.V) then yield

$$\Gamma_{sp} = \frac{2\pi}{\hbar}\int \mathrm{d}^2k \exp(-2\tilde{p}z)\left|\mathbf{D}_{fi}\cdot(\hat{\mathbf{z}}k - \mathrm{i}\hat{\mathbf{k}}\tilde{p})\right|^2 \delta(E_{if} - \hbar\Omega(k)). \tag{C.11}$$

With the integrand re-expressed as a function of $\tilde{p}$, the delta function prescribes $\Omega = E_{if}/\hbar$, and eventually one finds

$$\begin{aligned}
&\tilde{p} = \frac{\Omega^2}{c^2 q} = \frac{E_{if}^2}{\hbar^2 c^2 q},\\
&\Gamma_{sp} = 2\pi \mathrm{e}^{-2\tilde{p}z}\left(\frac{E_{if}}{\hbar c}\right)^4 \frac{1}{q\hbar}\left\{D_{zfi}^2\left[\left(\frac{E_{if}}{\hbar c q}\right)^2 + 1\right] + \frac{1}{2}\mathbf{D}_{\|fi}^2\left(\frac{E_{if}}{\hbar c q}\right)^2\right\}.
\end{aligned} \tag{C.12}$$

Since E_{if} and the matrix elements are fixed, the PR limit, via $q\to\infty$, entails $\tilde{p}\to 0$. This appears to make the rate independent of z, and a paradox is avoided only because in fact Γ_{sp} vanishes (even when $z = 0$):

$$\Gamma_{sp} \to 2\pi\left(\frac{E_{if}}{\hbar c}\right)^4 \frac{1}{q\hbar} D_{zfi}^2 \to 0. \tag{C.13}$$

Appendix D. The nonretarded model

This model was introduced in BV, appendix B; here we study only its field-energy density u_{NR}. We recall $\Omega_{NR} = c^2 q k$, and start under a cutoff, as did appendix C:

$$8\pi u_{NR}(z) = \hbar c\sqrt{q}\left(\frac{K}{Z}\right)^{7/2}\mathcal{I}_{NR}(Z), \qquad \mathcal{I}_{NR}(Z) \equiv \int_0^Z \mathrm{d}y\, y^{5/2}\exp(-y), \tag{D.1}$$

$$\mathcal{I}_{NR}(Z) = \frac{15\sqrt{\pi}}{8}\mathrm{erf}(\sqrt{Z}) - \exp(-Z)\left[\frac{15}{4}Z^{1/2} + \frac{5}{2}Z^{3/2} + Z^{5/2}\right], \tag{D.2}$$

$$\mathcal{I}_{NR}(Z\to 0) = \frac{2}{7}Z^{7/2} - \frac{2}{9}Z^{9/2} + \mathcal{O}(Z^{11/2}), \tag{D.3}$$

$$\mathcal{I}_{NR}(Z\to\infty) = 15\pi^{1/2}/8 + \mathcal{O}(\mathrm{e}^{-Z}Z^{5/2}). \tag{D.4}$$

The no-cutoff limit evidently reads

$$u_{NR}^{(NC)}(z) \equiv \lim_{K\to\infty} u_{NR}(z), \qquad 8\pi u_{NR}^{(NC)}(z) = \frac{\hbar c\sqrt{q}}{z^{7/2}}\frac{15\pi^{1/2}}{64\sqrt{2}}. \tag{D.5}$$

Without retardation it is especially easy to show that, while the kinetic energy κ_{NR} naturally resides on the sheet, the Coulomb energy $U_{NR} \equiv 2\int_0^\infty \mathrm{d}z u_{NR} = \beta_{NR} - \kappa_{NR}$ is concentrated within a distance of order a from the sheet[13]. We merely scale in the way already motivated in appendix C.2, i.e. energy to β_{NR} and the distance z to $1/2K = a/4\sqrt{\pi}$, so that the scaled distance becomes Z; and then write ρ_{NR} for the correspondingly scaled density of the field energy:

$$\rho_{NR} = \frac{u_{NR}}{2K\beta_{NR}} = \frac{5}{8}\frac{\mathcal{I}_{NR}(Z)}{Z^{7/2}}. \tag{D.6}$$

This proves the point in virtue simply of the fact that ρ_{NR} depends on z only through Z.

In fact the conclusion could have been anticipated dimensionally, given that, by construction, both β and u are proportional to $\hbar$. Because the only other NR input parameters are a, e^2 and m, one must have $\beta_{NR} \sim \hbar\sqrt{e^2/ma^7}$ and $u_{NR} \sim \hbar\sqrt{e^2/mz^5}g(z/a)$, with g a dimensionless function of its dimensionless argument; whence $\rho_{NR} \sim au_{NR}/\beta_{NR} \sim g(z/a)(z/a)^{-5/2}$, a function only z/a, as claimed.

Appendix E. $\langle \mathbf{E}^2\rangle$ and $\langle \mathbf{B}^2\rangle$ under cutoff

E.1. Preliminaries

We consider only the realistic regime where $X \gg 1$ (which excludes formally near-perfect reflection), and recall $Z = X\zeta$. Further, we shall concentrate on small Z (where *a fortiori* $\zeta = Z/X \ll 1$), because (i) cutofff dependence at arbitrary Z is extremely tedious both to calculate and to display; while (ii) it will appear presently that, as anticipated in section 1, for large Z the cutoff makes only a negligible difference, of relative order $\exp(-Z)$. Accordingly, and so as to avoid intolerable complication, we aim to be accurate only up to terms that vanish as *Z and/or $1/X$ tend to zero*. Of course one must bear in mind that, with or without cutoff, for the fields at $z \lesssim a$, i.e. at $\zeta = 2\pi qa \sim \alpha^2 \sim 10^{-4}$, the detailed assertions of our continuum model are indicative at best, because the physics then depends appreciably on the microscopic (hence granular) structure of the material.

Starting with the photon modes, one allows for the sp modes by dropping the pole contribution to a TM contour integral in the complex p plane, much as in section 3.3. We settle for a very rough outline of the TE calculation, with the TM results merely quoted.

The integration variables k and p are scaled to y, x as before, but rather than focus on the form factors $\mathcal{J}$ defined as in section 3, we now write

$$\langle \mathbf{E}^2\rangle = \frac{\hbar c q^4}{\pi}\mathcal{F}_E, \qquad \mathcal{F}_E = (\pi/\zeta^4)\mathcal{J}_E, \tag{E.1}$$

$$\mathcal{F}_E = \left\{\int_0^\infty \mathrm{d}x\int_0^x \mathrm{d}y - \int_X^\infty \mathrm{d}x\int_X^x \mathrm{d}y\right\}\exp(-\zeta x) f_E(x, y) \equiv \mathcal{F}_{ENC} - \mathcal{F}_{E3}, \tag{E.2}$$

and similarly for $\langle \mathbf{B}^2\rangle$. The $f_{E,B}$ are algebraic functions; $f_E^{TE,TM}$, say, are identifiable from (3.8) and from (3.16). Evidently $\mathcal{F}_{\mathrm{NC}}$ is the no-cutoff result, while $\mathcal{F}_3$ subtracts the

[13] The corresponding argument for a spherical shell, as laid out in section 3.2 of B.IV, mis-identifies the range of radial distances where it applies; also it suffers from an algebraic slip. The corrections are given in an erratum (Barton 2004c), which shows that the original conclusions are nevertheless substantially correct.

contributions from the modes having $k > K$, which are eliminated by the cutoff. To exploit this subdivision, one splits the pertinent part $y < x$ of the positive quadrant of the xy plane into three: region 1 with $(x < X, y < x)$, region 2 with $(x > X, y < X)$ and region 3 with $(x > X, X < y < x)$. Without a cutoff the integral runs over all three regions (i.e. $\mathcal{F}_{\rm NC} = \mathcal{F}_1 + \mathcal{F}_2 + \mathcal{F}_3$); with a cut-off it runs only over regions 1 and 2 ($\mathcal{F} = \mathcal{F}_1 + \mathcal{F}_2 = \mathcal{F}_{\rm NC} - \mathcal{F}_3$). Numerically, and especially at small distances, one might prefer to work with $\mathcal{F}_1 + \mathcal{F}_2$, which avoids expressions that diverge as $\zeta \to 0$; but analytically $\mathcal{F}_3$ proves more accessible.

Changing integration variables to $(\xi, \eta) \equiv (x/X, y/X)$, so that $\int_X^x \mathrm{d}y \exp(-\zeta x) \cdots = X \int_1^\xi \mathrm{d}\eta \exp(-Z\eta) \ldots$, we see at once that for large Z all cutoff-dependent terms are indeed small to the tune of $\exp(-X\zeta) = \exp(-Z)$, as claimed above.

E.2. Results

From (3.8) for $\mathcal{F}^{TE}_{ENC}$ and from (E.2) one obtains

$$\mathcal{F}^{TE}_{E3} = \int_X^\infty \mathrm{d}x \int_X^x \mathrm{d}y \frac{\exp(-\zeta x)}{x+1} y\sqrt{x^2-y^2} = X^3 \exp(Z/X) \int_Z^\infty \mathrm{d}\xi \exp(-\xi/X) \frac{K_2(\xi)}{\xi^2}. \tag{E.3}$$

Recall $K_2(\xi \to 0) \simeq 2/\xi^2$ and $K_2(\xi \to \infty) \simeq \sqrt{\pi/2}\exp(-\xi)$.

What interests us here is the regime where not only $\zeta \ll 1$ but also $Z \lesssim \mathcal{O}(1)$, and especially the limit $Z \to 0$. Then the integral is dominated by moderate values of ξ, so that one can expand

$$\exp(-\xi/X) \simeq 1 - \xi/X + \xi^2/2X^2 - \xi^3/6X^3 + \cdots \tag{E.4}$$

and integrate term by term. The essential points are (a) that (E.4) is an expansion by powers of $1/X$, and (b) that the terms dropped from (E.4) contribute to (E.3) only integrals that would converge if extended down to $\xi = 0$. Hence, in view of the factor X^3 of (E.3), and accurately up to terms that vanish as $X \to \infty$, one need keep only the four terms actually spelled out in (E.4). It is a further bonus that the integrals in question are all trivial to approximate for small Z. We evaluate them, substitute them into (E.3), re-expand in powers of Z, and finally express the result in terms of ζ and X (instead of Z and X). Then one finds

$$\begin{aligned}\mathcal{F}^{TE}_{E3} = {} & \frac{2}{3\zeta^3} - \frac{1}{3\zeta^2} - \left[\frac{X^2}{2} - \frac{1}{3}\right]\frac{1}{\zeta} - \frac{1}{2}X^2\left[\log\left(\frac{X\zeta}{2}\right) + \gamma\right] \\ & + \frac{1}{3}\left[\log\left(\frac{X\zeta}{2}\right) + \gamma\right] + \left[\frac{\pi}{6}X^3 - \frac{1}{4}X^2 - \frac{\pi}{4}X + \frac{4}{9}\right] + \mathcal{O}(\zeta\log(\zeta)) + \mathcal{O}(X^{-1}).\end{aligned} \tag{E.5}$$

According to (E.2) this must be subtracted from

$$\mathcal{F}^{TE}_{ENC}(\zeta \to 0) = \frac{1}{3}\left\{\frac{2}{\zeta^3} - \frac{1}{\zeta^2} + \frac{1}{\zeta} + \log(\zeta) + \gamma\right\} + \mathcal{O}(\zeta\log(\zeta), \tag{E.6}$$

obtainable from (3.12). The terms with ζ^{-3}, ζ^{-2} and with ζ^{-1} and $\log(\zeta)$ but without X cancel, and the end result reads

$$\mathcal{F}^{TE}_{E} \simeq \frac{X^2}{2\zeta} - X^3\frac{\pi}{6} + X^2\left[\frac{1}{2}\log\left(\frac{Z}{2}\right) + \frac{\gamma}{2} + \frac{1}{4}\right] + X\frac{\pi}{4} + \log\left(\frac{X}{2}\right) - \frac{4}{9}. \tag{E.7}$$

Parallel calculations yield

$$\mathcal{F}^{TE}_{B} \simeq -\frac{X^2}{2\zeta} - X^3\frac{\pi}{6} - X^2\left[\frac{1}{2}\log\left(\frac{Z}{2}\right) + \frac{\gamma}{2} - \frac{3}{4}\right] - X\frac{3\pi}{4} + \frac{14}{9}, \tag{E.8}$$

$$\mathcal{F}_E^{TMt} \simeq \frac{X^2}{2\zeta} + X^{7/2}\frac{2\pi}{7} - X^3\frac{11}{12} + X^{5/2}\frac{\pi}{5} + X^2\left[\frac{1}{2}\log(Z) + \frac{\gamma}{2} + \frac{1}{48}\right] + X\frac{13}{30} + \frac{1233}{4900}, \tag{E.9}$$

$$\mathcal{F}_B^{TMt} \simeq -\frac{X^2}{2\zeta} + X^{5/2}\frac{\pi}{5} - X^2\left[\frac{1}{2}\log(Z) + \frac{\gamma}{2} + \frac{15}{64}\right] - X\frac{25}{48} + \frac{311}{800}. \tag{E.10}$$

Thus

$$\mathcal{F}_E \equiv \mathcal{F}_E^{TE} + \mathcal{F}_E^{TMt} = \frac{X^2}{\zeta} + X^{7/2}\frac{2\pi}{7} + \mathcal{O}(X^3), \tag{E.11}$$

$$\mathcal{F}_B \equiv \mathcal{F}_B^{TE} + \mathcal{F}_B^{TMt} = -\frac{X^2}{\zeta} + \mathcal{O}(X^3). \tag{E.12}$$

In contrast, from the combinations $\mathcal{F}_u^{TE} \equiv \mathcal{F}_E^{TE} + \mathcal{F}_B^{TE}$ and $\mathcal{F}_u^{TMt} \equiv \mathcal{F}_E^{TMt} + \mathcal{F}_B^{TMt}$ the terms proportional X^2/ζ cancel.

E.3. Comments

- It is only at large ζ, where the *dispersive* corrections have become negligible, that $\langle\mathbf{E}^2\rangle$ becomes directly measurable through the Casimir–Polder potential V_{CP} from (1.3). But then, *a fortiori*, $Z \gg 1$, so that the cutoff has become irrelevant as well.
- No paradox attaches to the fact that even under the cutoff $\langle\mathbf{E}^2\rangle$ and $\langle\mathbf{B}^2\rangle$ diverge as $z \to 0$, because these mean-square fields include contributions from the self-fields of the fluid. Indeed, in the present context it matters little whether the energy density $u = \langle\mathbf{E}^2 + \mathbf{B}^2\rangle/8\pi$ is likewise divergent; nor even whether it is integrable.
- In fact, (E.11), (E.12) yield

$$\mathcal{F}_u \equiv \mathcal{F}_E + \mathcal{F}_B = X^{7/2}\frac{2\pi}{7} + \mathcal{O}(X^3)\,: \tag{E.13}$$

  the terms featuring $\pm X^2/2\zeta$ have cancelled, so that $u = (\hbar c q^4/8\pi^2)\mathcal{F}_u$ does remain finite down to $z = 0$. Its leading term

$$\frac{hcq^4}{\pi}\mathcal{F}_u \simeq \frac{\hbar c q^{1/2} K^{7/2}}{4\pi\cdot 7} = \frac{\hbar K^{7/2}}{2}\sqrt{\frac{ne^2}{2\pi m}}$$

  tallies with (D.1), (D.3) from the NR model, though the writer sees no *a priori* reason why it should.
- Reverting to $\langle\mathbf{E}^2\rangle$, we see that as ζ increases from zero, the initially divergent and therefore nominally dominant component $X^2/2\zeta$ is overtaken by the nonretarded component $2\pi X^{7/2}/7$ when $\zeta \sim X^{-3/2}$, which means $z \sim \sqrt{ar_0} = a\sqrt{r_0/a} \sim a\alpha = \lambda_c/2\pi \ll a$. In other words the possibly surprising retardation effects right next to the sheet are confined to a region so narrow that for any half-way practical purposes they are irrelevant.

Appendix F. Perfect reflectors

Perfect reflection at all frequencies, i.e. $\mathcal{T}^{(+)} \to 0, \mathcal{R}^{(+)} \to -1$, requires $q \to \infty$, so that $X \to 0$. In our model this scenario is unrealistic; nevertheless it is of some formal interest, because it is so widely discussed, and because the limit presents paradoxes that, undiagnosed, have caused confusion. One example appears at the end of appendix F.1.2, and another in appendix F.2.

F.1. Perfect reflection ab initio

F.1.1. Without cutoff. Here one starts with the familiar expansions, in the half-space $z > 0$, of fields that are subject from the outset to the perfect-reflector boundary conditions

$$\mathbf{E}_{\parallel}^{(\mathrm{PR})} = 0, \qquad B_z^{(\mathrm{PR})} = 0 \qquad (z = 0).$$

Then one sees no surface modes, and, adapting the notation of section 2.2 of B.V one has[14]

$$\mathbf{F}^{(\mathrm{PR})j} = \int \mathrm{d}^2k \int_0^\infty \mathrm{d}p \sqrt{\frac{\hbar\omega}{\pi^2 k^2}} a_{\mathbf{k},p}^{(\mathrm{PR})j} \mathbf{F}_{\mathbf{k},p}^{(\mathrm{PR})j} + Hc, \tag{F.1}$$

$$\begin{aligned}\left(\mathbf{E}_{\mathbf{k},p}^{(\mathrm{PR})TE}, \mathbf{B}_{\mathbf{k},p}^{(\mathrm{PR})TE}, \mathbf{E}_{\mathbf{k},p}^{(\mathrm{PR})TM}, \mathbf{B}_{\mathbf{k},p}^{(\mathrm{PR})TM}\right) &= \exp(-\mathrm{i}\omega t + \mathrm{i}\mathbf{k}\cdot\mathbf{s}) \\ &\times \begin{pmatrix} \mathrm{i}(\hat{\mathbf{k}}\times\hat{\mathbf{z}})k\sin(pz) \\ (ck/\omega)\{-\mathrm{i}\hat{\mathbf{z}}k\sin(pz) + \hat{\mathbf{k}}p\cos(pz)\} \\ (ck/\omega)\{-\mathrm{i}\hat{\mathbf{z}}k\cos(pz) - \hat{\mathbf{k}}p\sin(pz)\} \\ -\mathrm{i}(\hat{\mathbf{k}}\times\hat{\mathbf{z}})k\cos(pz) \end{pmatrix}, \qquad (z > 0).\end{aligned} \tag{F.2}$$

The amplitudes are $\sqrt{2}$ times those of the odd-parity modes: appendix F.2 explains why.

The reader should be warned straightaway that, as regards the physics of imperfect reflectors, one is badly misled by almost every qualitative conclusion that it might seem plausible to infer from (F.2).

The zero-point mean-square fields follow at once. Defining

$$\nu \equiv \sqrt{k^2 + p^2}$$

we find

$$\begin{aligned}&\left(\langle\mathbf{E}^2\rangle_{TE}, \langle\mathbf{B}^2\rangle_{TE}, \langle\mathbf{E}^2\rangle_{TM}, \langle\mathbf{B}^2\rangle_{TM}\right) \\ &\qquad = 2\pi \int_0^\infty \mathrm{d}k\, k \int_0^\infty \mathrm{d}p \frac{\hbar c\nu}{\pi^2 k^2} \begin{pmatrix} k^2\sin^2(pz) \\ (k/\nu)^2[k^2\sin^2(pz) + p^2\cos^2(pz)] \\ (k/\nu)^2[k^2\cos^2(pz) + p^2\sin^2(pz))] \\ k^2\cos^2(pz) \end{pmatrix} \\ &\qquad \to \frac{\hbar c}{\pi} \int_0^\infty \mathrm{d}k k \int_0^\infty \mathrm{d}p \cos(2pz)(-\nu, (p^2 - k^2)/\nu, -(p^2 + k^2)/\nu, \nu),\end{aligned} \tag{F.3}$$

where the arrow replaces $(\cos^2(pz), \sin^2(pz)) \to \pm\cos(2pz)/2$, dropping terms that are independent of z, and are therefore cancelled when one subtracts the mean-square fields in the absence of the mirror. Ahead of any integrations, one sees that

$$\langle\mathbf{E}^2\rangle_{TM}^{(\mathrm{PR})} = -\langle\mathbf{B}^2\rangle_{TE}^{(\mathrm{PR})}, \qquad \langle\mathbf{B}^2\rangle_{TM}^{(\mathrm{PR})} = -\langle\mathbf{E}^2\rangle_{TE}^{(\mathrm{PR})}. \tag{F.4}$$

For perfect reflectors it will therefore suffice to display only the TE expressions.

There are several ways of evaluating these expectation values. The traditional method, not readily adapted to a cutoff, reverses the order of integration, replaces $\int_0^\infty \mathrm{d}k k \ldots \to \int_p^\infty \mathrm{d}\nu\nu \ldots$, and then, as symbolized by another arrow, drops the contributions from the upper limit because, being independent of p (although divergent[15]) they yield only terms proportional

[14] In this section we drop the labels (PR), except from end results.

[15] In fact the word 'although' is misleading, because it is precisely their divergence that makes these terms independent of p.

to $\int_0^\infty \mathrm{d}p\cos(2pz) = (\pi/2)\delta(z)$, which vanish everywhere off the sheet. This yields

$$\begin{aligned}\big(\langle\mathbf{E}^2\rangle, \langle\mathbf{B}^2\rangle\big)_{TE}^{(\mathrm{PR})} &= \frac{\hbar c}{\pi}\int_0^\infty \mathrm{d}p\cos(2pz)\int_p^\infty \mathrm{d}\nu(-\nu^2, -\nu^2+2p^2),\\ \begin{pmatrix}\langle\mathbf{E}^2\rangle\\ \langle\mathbf{B}^2\rangle\end{pmatrix}_{TE}^{(\mathrm{PR})} &\to \frac{\hbar c}{\pi}\int_0^\infty \mathrm{d}p\cos(2pz)p^2\frac{1}{3}\begin{pmatrix}1\\-5\end{pmatrix} = \frac{\hbar c}{8\pi z^4}\begin{pmatrix}1\\-5\end{pmatrix}.\end{aligned} \tag{F.5}$$

The last step uses an identity standard for generalized functions, namely

$$\int_0^\infty \mathrm{d}p\cos(2pz)p^3 = -\frac{1}{8}\frac{\partial^3}{\partial z^3}\int_0^\infty \mathrm{d}p\sin(2pz) = -\frac{1}{8}\frac{\partial^3}{\partial z^3}\left(\frac{1}{2z}\right) = \frac{3}{8z^4}.$$

Accordingly[16]

$$\begin{pmatrix}\langle\mathbf{E}^2\rangle\\ \langle\mathbf{B}^2\rangle\end{pmatrix}^{(\mathrm{PR})} = \begin{pmatrix}\langle\mathbf{E}^2\rangle_{TE+TM}\\ \langle\mathbf{B}^2\rangle_{TE+TM}\end{pmatrix}^{(\mathrm{PR})} = \pm\frac{3\hbar c}{4\pi z^4} = \pm\frac{\hbar c q^4}{\pi}\frac{12}{\zeta^4}. \tag{F.6}$$

F.1.2. With cutoff. Equations (F.6) apply without a cutoff. With a cutoff we choose a more flexible method, which reverts to (F.3); replaces $\int_0^\infty \mathrm{d}p\cos(2pz)\ldots \to (1/2)\mathrm{Re}\int_{-\infty}^\infty \mathrm{d}p\exp(\mathrm{i}2pz)\ldots$; and (for $z>0$) closes the contour in the upper-half complex p plane, with a hair-pin detour around the cut (due to ν) from $p=\mathrm{i}k$ to $\mathrm{i}\infty$. On the right and left of the cut, where $p=\mathrm{i}y\pm 0$, we have $\nu = \pm\mathrm{i}\sqrt{y^2-1}$. Scaling via $y=kx$, one readily finds

$$\begin{aligned}\langle\mathbf{E}^2, \mathbf{B}^2\rangle_{TE} &= \frac{\hbar c}{\pi}\int_0^K \mathrm{d}k\,k^3\int_1^\infty \mathrm{d}x\exp(-2kzx)\big(\sqrt{x^2-1}, -\big[\sqrt{x^2-1}+2/\sqrt{x^2-1}\big]\big)\\ &= \frac{\hbar c}{\pi}\int_0^K \mathrm{d}k\,k^3\left(K_1(2kz)/2kz, -\left[K_1(2kz)/2kz + 2K_0(2kz)\right]\right),\end{aligned}$$

where we have used

$$\int_1^\infty \mathrm{d}t\exp(-\xi t)(t^2-1)^{n-1/2} = \frac{\Gamma(n+1/2)}{\sqrt{\pi}}\left(\frac{2}{\xi}\right)^n K_n(\xi). \tag{F.7}$$

The remaining integrals are elementary, and the end results, formatted to match (F.5), read

$$\begin{pmatrix}\langle\mathbf{E}^2\rangle\\ \langle\mathbf{B}^2\rangle\end{pmatrix}_{TE}^{(\mathrm{PR})} = \frac{\hbar c}{8\pi z^4}\begin{pmatrix}[1-Z^2K_2(Z)/2]\\ -[5-5Z^2K_2(Z)/2 - Z^3K_1(Z)]\end{pmatrix}, \tag{F.8}$$

whence

$$\begin{aligned}\langle\mathbf{E}^2\rangle^{(\mathrm{PR})} &= \langle\mathbf{E}^2\rangle_{TE+TM}^{(\mathrm{PR})} = \langle\mathbf{E}^2\rangle_{TE}^{(\mathrm{PR})} - \langle\mathbf{B}^2\rangle_{TE}^{(\mathrm{PR})} = -\langle\mathbf{B}^2\rangle^{(\mathrm{PR})}\\ &= \frac{\hbar c}{8\pi z^4}\{6-3Z^2K_2(Z) - Z^3K_1(Z)\}.\end{aligned} \tag{F.9}$$

Since $Z\equiv 2Kz$, we see that $K\to\infty$ and $z\to 0$ are incompatible. For large Z, we have another illustration of the general fact that for large Z cutoff-dependent corrections vanish exponentially fast, i.e. proportionally to $\exp(-Z)$. For small Z,

$$\langle\mathbf{E}^2\rangle^{(\mathrm{PR})} = -\langle\mathbf{B}^2\rangle^{(\mathrm{PR})} = \frac{\hbar c K^2}{8\pi z^2}\left\{2+2(Kz)^2\left[\log\left(\frac{1}{Kz}\right) - \gamma - \frac{1}{4}\right] + \mathcal{O}(Kz)^4\right\}. \tag{F.10}$$

Finally we observe that, for perfect reflection and off the mirror, the total field-energy density of the photon modes vanishes, with or without a cutoff. This observation, and the common misidentification of the surface energy β with $2\int_0^\infty \mathrm{d}z u$, are probably responsible for the

[16] The rightmost expression is alien to perfect reflection (where $q\to\infty$), but fits our notation for dispersive sheets.

widespread delusion that the surface energy of perfect reflectors vanishes: whereas we already know from section 3.4 of B.V that, as the perfect-reflector limit is *approached*, i.e. as $q \to \infty$ at fixed K, one has $\beta \simeq -(\hbar c q K^2/4\pi^2)\log(2q/K)$, which tends not to zero but to $-\infty$.

F.2. Perfect reflection as a limit

We conclude by showing that the perfect-reflector limit turns the left-hand and the right-hand half-spaces into electromagnetically disjoint and quantally independent systems, with a direct-product overall Hilbert space. Though this could perhaps be regarded as an intuitively obvious consequence of separation by a perfect mirror, in our model it might appear paradoxical, because the odd-parity (half the total) normal modes know nothing of q, and are therefore unaffected as $q \to \infty$. The paradox, if it is one, was anticipated at the end of section 2.1 in B.V, and is resolved automatically by proving the disjuncture.

The proof starts by noting that $q \to \infty$ entails

$$\eta, \mu \to -\pi/2 \Rightarrow \begin{pmatrix} \cos(pz + (\eta, \mu)) \\ \sin(pz + (\eta, \mu)) \end{pmatrix} \to \begin{pmatrix} \sin(pz) \\ -\cos(pz) \end{pmatrix}. \tag{F.11}$$

Thus for $z > 0$ the even-parity (interacting) photon modes become identical to the corresponding odd-parity (noninteracting) modes[17]. This allows one to change (unitarily transform to) new modes labelled R, L, whose annihilation operators and amplitudes are

$$a^{(R,L)}_{\mathbf{k},p} = \left(a^{(+)}_{\mathbf{k},p} \pm a^{(-)}_{\mathbf{k},p}\right)/\sqrt{2}, \qquad \left[a^{(R)+}_{\mathbf{k},p}, a^{(L)}_{\mathbf{k},p}\right] = 0, \qquad \mathbf{F}^{(R,L)}_{\mathbf{k},p} = \left(\mathbf{F}^{(+)}_{\mathbf{k},p} \pm \mathbf{F}^{(-)}_{\mathbf{k},p}\right)/\sqrt{2}, \tag{F.12}$$

where for simplicity we have suppressed the polarization index.

For $z > 0$, the new modes $\mathbf{F}^{(R)}_{\mathbf{k},p} = \sqrt{2}\mathbf{F}^{(-)}_{\mathbf{k},p}$ are precisely those that one introduces when quantizing the Maxwell field to the right of a perfectly reflecting surface (see, e.g., Barton (1974)), with no questions asked about any physics to its left. This is the origin of the factor $\sqrt{2}$ remarked on just below (F.2).

References

Babiker M and Barton G 1976 *J. Phys. A: Math. Gen.* **9** 129
Barton G 1974 *J. Phys. B: At. Mol. Phys.* **7** 2134
Barton G 1977 *J. Phys. A: Math. Gen.* **10** 601
Barton G 1989 *Phys. Rev.* D **40** 4096
Barton G 1991a *J. Phys. A: Math. Gen.* **24** 991
Barton G 1991b *J. Phys. A: Math. Gen.* **24** 5533
Barton G 2001a *J. Phys. A: Math. Gen.* **34** 4083
Barton G 2001b *J. Phys. A: Math. Gen.* **34** 5781
Barton G 2002 *Int. J. Mod. Phys.* A **17** 767
Barton G 2004a *J Phys A: Math. Gen.* **37** 1011 (referred to as B.III)
Barton G 2004b *J Phys A: Math. Gen.* **37** 3725 (referred to as B.IV)
Barton G 2004c *J. Phys. A: Math. Gen.* **37** 11945 (erratum)
Barton G 2005 *J. Phys. A: Math. Gen.* **38** 2997 (referred to as B.V)
Bordag M 2004 *Phys. Rev.* D **70** 085010
Eberlein C and Robaschik D 2004 *Phys. Rev. Lett.* **92** 233602
Graham N, Olum K D and Schwartz-Perlov D 2004 *Phys. Rev.* D **70** 105019

[17] If one first imposes auxiliary (say periodic) boundary conditions on the fields at $z = \pm L$, so that p discretizes to $p_n = n\pi/L$ (with non-negative integer n), then as $L \to \infty$ one sees that $q \to \infty$ actually assimilates even-parity modes having given n to odd-parity modes having not the same but adjacent values of n.

Helfer A D and Lang S I D 1999 *J. Phys. A: Math. Gen.* **32** 1937
Hinds E A 1994 *Cavity Quantum Electrodynamics* ed P R Berman (Boston, MA: Academic)
Landragin A, Courtois J-Y, Labeyrie G, Vansteenkiste N, Westbrook C I and Aspect A 1996 *Phys. Rev. Lett.* **77** 1464
Maddox J 1993 *Nature* **361** 493
Robaschik D and Wieczorek E 1994 *Ann. Phys. NY* **236** 43
Sandoghdar V, Sukenik C I, Haroche S and Hinds E A 1996 *Phys. Rev.* A **53** 1919
Sopova V and Ford L H 2002 *Phys. Rev.* D **66** 045026
Sukenik C I, Boshier M G, Cho D, Sandoghdar V and Hinds E A 1993 *Phys. Rev. Lett.* **70** 560